Introduction to Research in Magnetic Resonance Imaging

Fábio Augusto Menocci Cappabianco, Claudio Saburo Shida
Department of Science and Technology
Federal University of São Paulo
São José dos Campos
http://gibis.unifesp.br

Jaime Shinsuke Ide
Department of Biomedical Engineering
Stony Brook University
Stony Brook, NY 11794, USA

***Abstract*—The advent of magnetic resonance imaging (MRI) and functional magnetic resonance imaging (fMRI) of the brain has changed forever conventional patient diagnosis and treatment in medicine. Instead of employing invasive procedures, now physicians can not just literally see internal body structures but also understand and map more clearly brain functions related to specific tasks, feelings, and behaviors. This paper aims at introducing the acquisition process, image processing, analysis and evaluation, and the most popular tools for both structural MRI and fMRI. It is an opportunity for students and researchers who are interested in getting started in the area, understanding what are the challenges and unexplored fields, and how to avoid the most common traps and pitfalls.**

***Keywords*-magnetic resonance imaging, functional magnetic resonance imaging, brain**

I. Introduction

The objective of this paper is to introduce students and researchers to MRI and fMRI. It will cover the acquisition process, image processing and analysis techniques, the evaluation methodologies, and the most popular tools for both structural MRI and fMRI. It is an opportunity for those who are interested in getting started in the area, understanding what are the challenges and unexplored fields, and how to avoid the most common traps and pitfalls. Even though we will focus on brain MRI, the concepts also apply to scans from other body parts.

MRI related discoveries rendered several Nobel Prizes, including the one in 2003 for magnetic resonance imaging (MRI) [1], [2]. Its importance is unquestionable due to its application on health care. Structural MRI consists of 3D images that allow physicians to literally look inside the patients body for disease diagnosis [3][4][5], treatment planning [6], and to monitor the recovery from surgeries [7]. Two decades ago, functional magnetic resonance imaging (fMRI), which is a time series of 3D images, extended the range of brain imaging applications since it enabled the understanding of behavioral, social, and psychological aspects of diseases, and relate them with neuro activations of specific brain regions [8][9][10].

MRI, which is an application of Nuclear Magnetic Resonance phenomena, is generated based on the response of hydrogen nuclei spin, in a strong magnetic field, to electromagnetic radio wave pulses. The relaxation time of nuclear spin perturbation, after the radio wave pulse, is used to estimate the concentration of hydrogen atoms and differentiate tissues in small volumes of the scanned body denominated voxels [11]. Figure 1 shows MRI synthetic brain slices from BrainWeb dataset[1][12] in modalities T1- and T2-weighted relaxation times, and proton density (PD) that are among the most commonly used for brain structure study and exams. fMRI acquisition follows a similar idea. Instead of estimating the hydrogen atoms concentration, fMRI contains an estimation of the blood oxygen level in a period of time in which the participant performs any kind of mental or motor tasks, depending on the brain function of interest [13]. Figure 2 shows sample slices of a fMRI in a given instant of time from 1000 Functional Connectomes Project[2], Baltimore Pekar, J.J./Mostofsky, S.H. database. As fMRI consists of a time series of $T2^*$ images, it requires longer acquisition time and have lower spatial resolution than MRI.

MRI processing on the other hand requires understanding of advanced concepts in image processing and computer vision. For instance, image intensity inhomogeneity correction, a problem described in Section III-B, may be solved using frequency filtering [14], [15], [16], surface fitting [17], [18], [19], [20], stochastic models [21], [22], [23], and energy minimization [24], [25]. Tissue segmentation (see Section IV-B) consists in labeling brain voxels into gray matter (GM), white matter (WM), and cerebral-spinal fluid (CSF). It can be obtained from thresholding [26], region growing [27], clustering [28], [29], supervised learning [30], [31], [32], [21], [33], [34], and deformable models [35], [36] based methodologies. Figure 3 shows the labels assigned to voxels in an axial slice of a T1-weighted MR image. Image registration, discussed in Section V-C, is essential for population studies and for fMRI analysis. It consists in standardizing the image space into a common domain such the one of a probabilistic template or atlas [21], [31], [27], [37], [38], [39], [40]. Figure 4 shows an example of an atlas with WM, GM, and CSF probabilities for each voxel.

With respect to MRI evaluation methods, there is no clear standard to be employed. Take as an example tissue segmentation problem. Employing a manual tissue classification, for

[1] $http://www.bic.mni.mcgill.ca/brainweb/$
[2] $http://fcon\_1000.projects.nitrc.org$

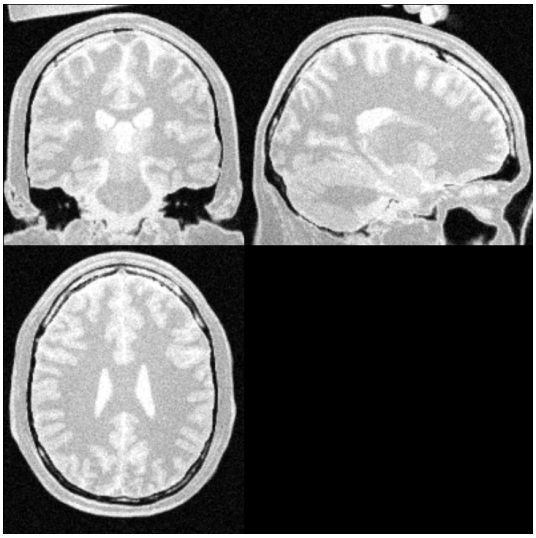

(a)

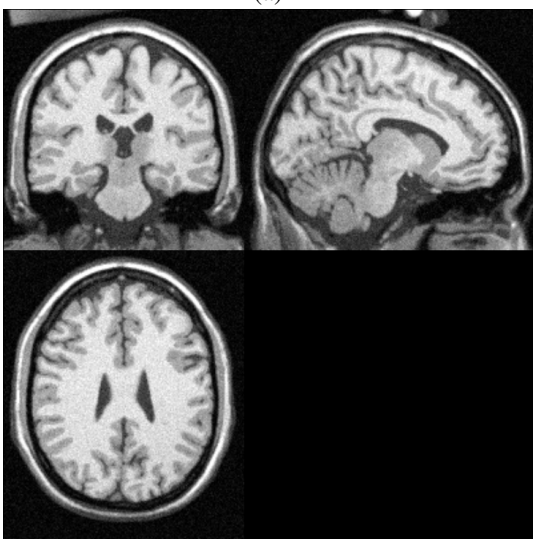

(b)

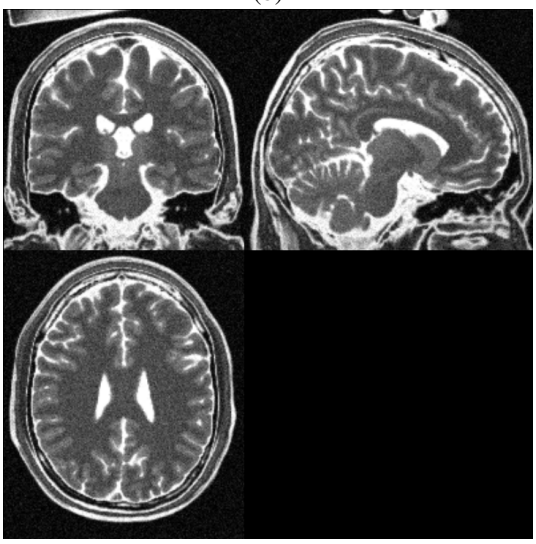

(c)

Fig. 1. Structural MRI slices in (a) PD, (b) T1-, and (c) T2-weighted modalities.

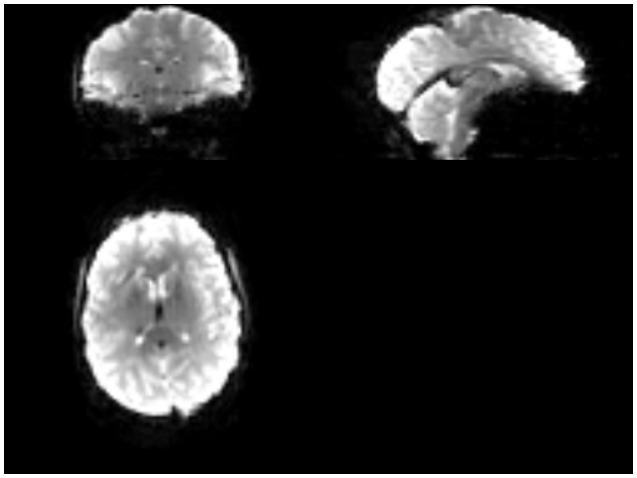

Fig. 2. Slices of a fMRI in a instant of time.

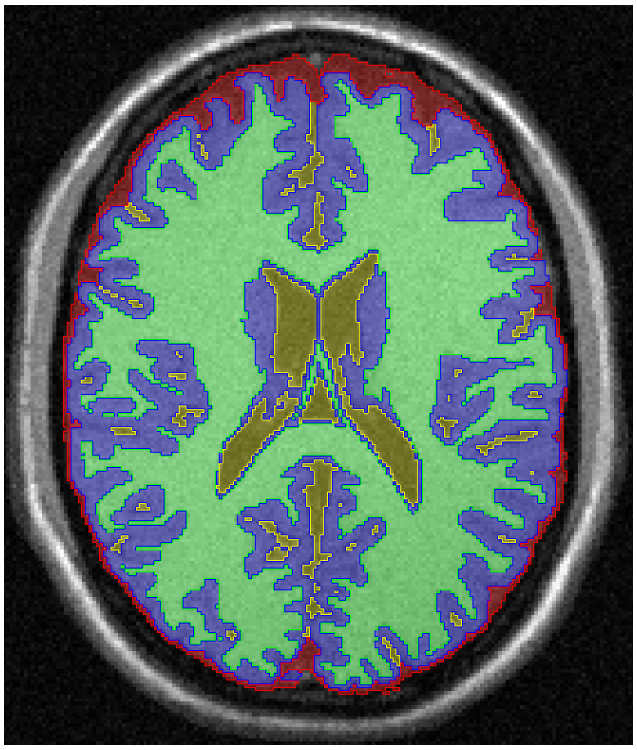

Fig. 3. Classification of tissues in MRI slice into internal and external cerebral-spinal fluid (yellow and red labels), gray and white matter (blue and green labels).

instance is a tedious and exhausting task prune to several errors [41]. Some semi-automatic methods were also used to generate a precise segmentation, but they may favor a specific class of method that is used in the classification procedure [31]. Also, synthetic images were constructed in order to have a perfect segmentation [12], but they do not reflect the same challenges faced when dealing with real images. The accuracy level of methods applied over such images tend to be much higher [38], [42].

fMRI have an even more complex experimental protocol.

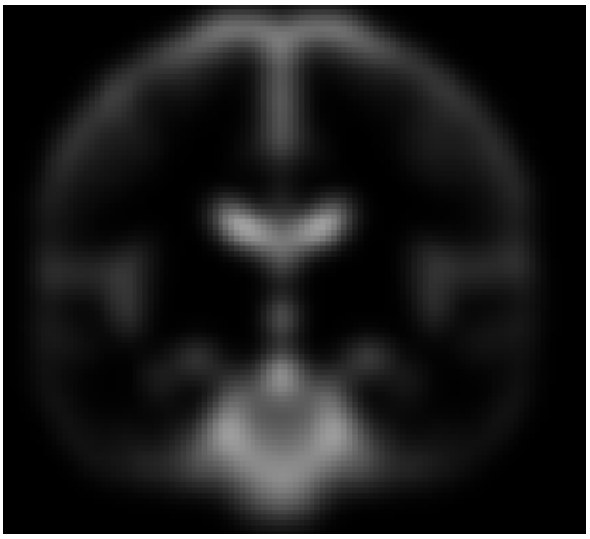

(a)

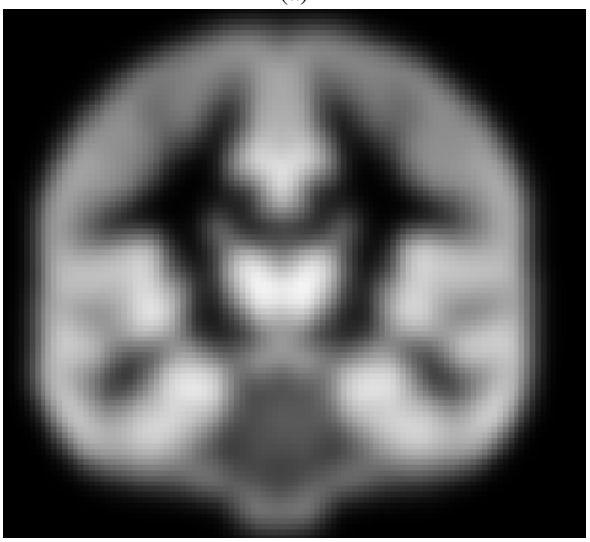

(b)

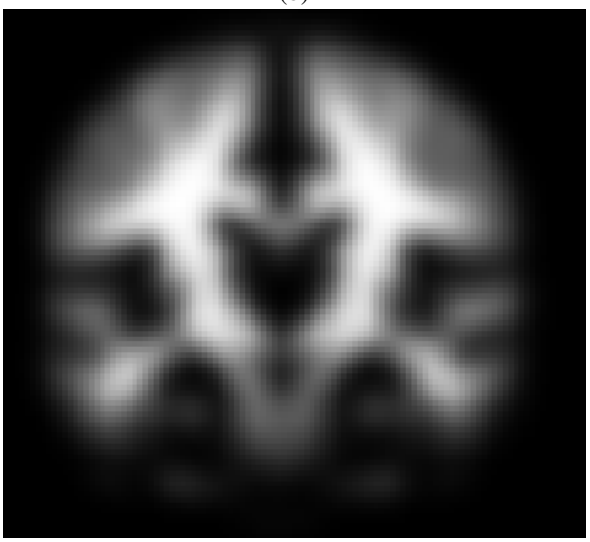

(c)

Fig. 4. Coronal slices of probabilistic atlas of (a) cerebro-spinal fluid, (b) gray matter, and (c) white matter.

The main goal is to estimate neural activity in a given area of the brain under specific situations. The two main classes of fMRI are the blood-oxygen-level dependent (BOLD) and the perfusion fMRI model [43] (see Section VI). The former reflects the total amount of deoxyhemoglobin that changes according to the hemodynamic response, that is, the dilation of blood vessels due to more intense neurological activities. The later is based on arterial spin labeling, a process in which arterial blood water flow is measured based on blood water magnetization with a 180 degree magnetic pulse in a specific brain area of interest, resulting in a reduced magnetization of the tissues that appear in the scanned images.

Two main approaches have being proposed for the analysis of fMRI data: the conventional mass-univariate approach known as general linear modeling (GLM) [44] and the multi-voxel pattern analysis (MVPA) using pattern recognition techniques [45], [46], [47] (see Sections VII-B and VIII-C, respectively). GLM, also known as encoding method, requires a priori task-design, and it generates a many-to-one mapping between experimental variables and one voxel [48]. MVPA techniques can be divided into decoding methods (many voxels to one experimental variable) and a more general multivariate many-to-many mapping. MPVA has the ability to delineate complex associations between multiple voxel, stimuli, and mental states in a data-driven way.

Therefore, this paper intends to give an introduction to MRI and fMRI acquisition, processing, analysis, and evaluation. It will serve as a guide for one who wants to start research in the area, giving directions and pointing most common traps and pitfalls.

II. The physical process of MRI acquisition

A. MRI fundamentals

MRI is a direct application of Nuclear Magnetic Resonance (NMR), a manifestation of quantum nature of matter. NMR phenomena was first observed in 1946 by Bloch [49] and Purcell *el al.* [50]. In 1952 they awarded the Nobel Prize for they contributions. However, the first MR image was only obtained by P.C. Lautenbur in 1973 [51]. Briefly we can say that NMR signal present in each voxel of 3D image is the response of hydrogen nuclei spin, in the presence of a strong magnetic field, to pulses of Radio Frequency (RF) wave.

To detect NMR signal, it is essential to have a scanned subject composed by atoms with nuclear spin, which is the intrinsic magnetic moment of nucleus. MRI of hydrogen is the most commonly used because this element is the most abundant isotope with nuclear spin in human body.

Over the years, two techniques of NMR have been developed: RF continuous wave and RF pulsed scanners. Today, all NMR scanners use the pulsed technique [52].

In MRI scanners a strong magnetic field is necessary to align the nuclear spin of hydrogen atoms. Once nuclear spins are aligned to the strong magnetic field, RF pulses are employed over them, disturbing and misaligning them from their equilibrium [53]. The return of these nucleus spins to equilibrium (relaxation) can be detected by coils perpendicular

to the applied external magnetic field [53]. Different relaxation times for different tissues, will give the intensity contrast of different tissues.

The relaxation time of nuclear spin perturbation, after the radio wave pulse, is also used to estimate the concentration of hydrogen atoms and differentiate tissues in small volumes of the brain denominated voxels [11]. Figure 1 shows the most common MRI modalities for brain studies: T1- and T2-weighted relaxation times, and PD. Different image contrasts in T1- and T2-weighted images can be obtained by changing the acquisition parameters of the RF pulses sequence applied. These RF pulse sequences parameters are: TE or echo time which represents the time from the center of the RF-pulse to the center of the echo; and, TR or repetition time that is the length of time between corresponding consecutive points on a repeating series of pulses and echoes. By changing values of TE and TR of a MRI scan, one can obtain T1-, T2-weighted or PD images with different contrasts [53].

MRI is a technique much more suited to image non-bony parts or soft tissue of the body than others tomographic scanners. The brain, spinal cord and nerves, as well as muscles, ligaments, and tendons are seen much more clearly with MRI than with regular x-rays and CT (Computadorized Tomography). This is the reason why MRI is used so often to image knee and shoulder injuries.

In the brain, MRI can differentiate between WM and GM and can also be used to diagnose aneurysms and tumors. Finally, MRI is the most appropriated choice for frequent imaging in diagnosis or therapy, especially involving the brain, because it does not use ionizing radiation present in x-ray exams. However, MRI is a more expensive procedure than others x-ray based techniques.

III. MRI INTENSITY REGULARIZATION

Even with all the advances in the acquisition process, MR images will probably present undesirable noise. Also, even images acquired using the same scanner and protocol may have considerable differences in the location of the region of interest, voxel intensity and contrast [54].

Therefore, it is of ultimate importance for any experiments to standardize the images before any procedure is executed. In this section we will present the procedures to normalize and to correct voxel and image intensity. In Section V, we discuss how to standardize voxel and image spatial domain.

A. High-frequency noise filtering

Filtering high frequency noise is important to accomplish tasks such as automatic tissue, organ, or region segmentation with higher accuracy. It is also indispensable for visualization purposes. Figure 5 shows the effect of noise with 3% and 9% of intensity amplitude over a coronal slice of T1, T2, and proton density (PD) synthetic images.

High-frequency noise in MRI are usually described as Johnson-Nyquist or thermal noise [55], [56]. It consists of an additive noise that follows a Rician distribution which may appear as Rayleigh and Gaussian distributions in regions with low and high signal-to-noise ratios (SNRs), respectively [32]. Therefore, most of the developed solutions filter MRI high frequency noise modeling it with Gaussian distribution.

The most common software used for high frequency noise filtering is the FMRIB Software Library (FSL) [3]. It contains a program called SUSAN [57] which consists of a local adaptive filter that preserves the image edges. BrainSuite [4] also provides an indirect way to get a local adaptive filter result by means of its Brain Surface Extractor (BSE) tool. Given an image of the brain, BSE was designed for skull and scalp removal, but it can also output the result of the execution of an anisotropic diffusion filter [58] over it. 3D Slicer [5] [59] also brings four kinds of filters including the traditional median, a Gaussian filter, a gradient and a curvature based anisotropic filters.

Currently, there is a new generation of non-local adaptive noise filters already tested on MRI [60], [61] but which is not in the core of any popular MRI processing packages. The main reason for that is probably because the new generation of scanners with higher magnetic field (e.g. 7 Tesla) has a very high SNR. Nevertheless, this is not the reality of all research centers, specially the ones in developing countries. The authors of Fast Nonlocal Means [6], a non-local filter for MRI suggest its use with 3D Slicer. The Biomedical Image Analysis Library [7] will soon offer an implementation of 3D non-local means filter as well [62].

B. Removing low-frequency noise - inhomogeneity effect

Low frequency noise is referred to as inhomogeneity effect or field, intensity or image non-uniformity, bias field, and by other similar terms. It consists of a shade like effect that enhances the intensity of a region in detriment of others. It has been most commonly modeled as a multiplicative effect over original data which is then corrupted by high frequency noise. Nevertheless, it is also presented by some authors as a multiplicative effect over the image already corrupted by high frequency noise [63].

Figure 6 shows a sagittal slice of a T1-weighted image which suffers from high inhomogeneity effect. Even though inhomogeneity may not affect a human expert analysis, for research and automatic procedures it is extremely important to correct or at least model it. Again any segmentation procedures or intensity based analysis may suffer considerable imprecision in the presence of intensity non-uniformity [64].

Bias field is a result of several factors related to the scanner, including poor radio frequency and eddy currents. These factors may be corrected or attenuated prior to image acquisition by scanning a phantom subject as a reference. Other factors are not related to the machine itself, but may arise from the patient anatomy and environment [54]. For the later cases, post image correction procedures are required.

[3] http://fsl.fmrib.ox.ac.uk/fsl/fslwiki/FSL
[4] http://brainsuite.org
[5] https://www.slicer.org/
[6] https://www.nitrc.org/projects/unlmeans/
[7] https://github.com/GIBIS-UNIFESP/BIAL-GUI

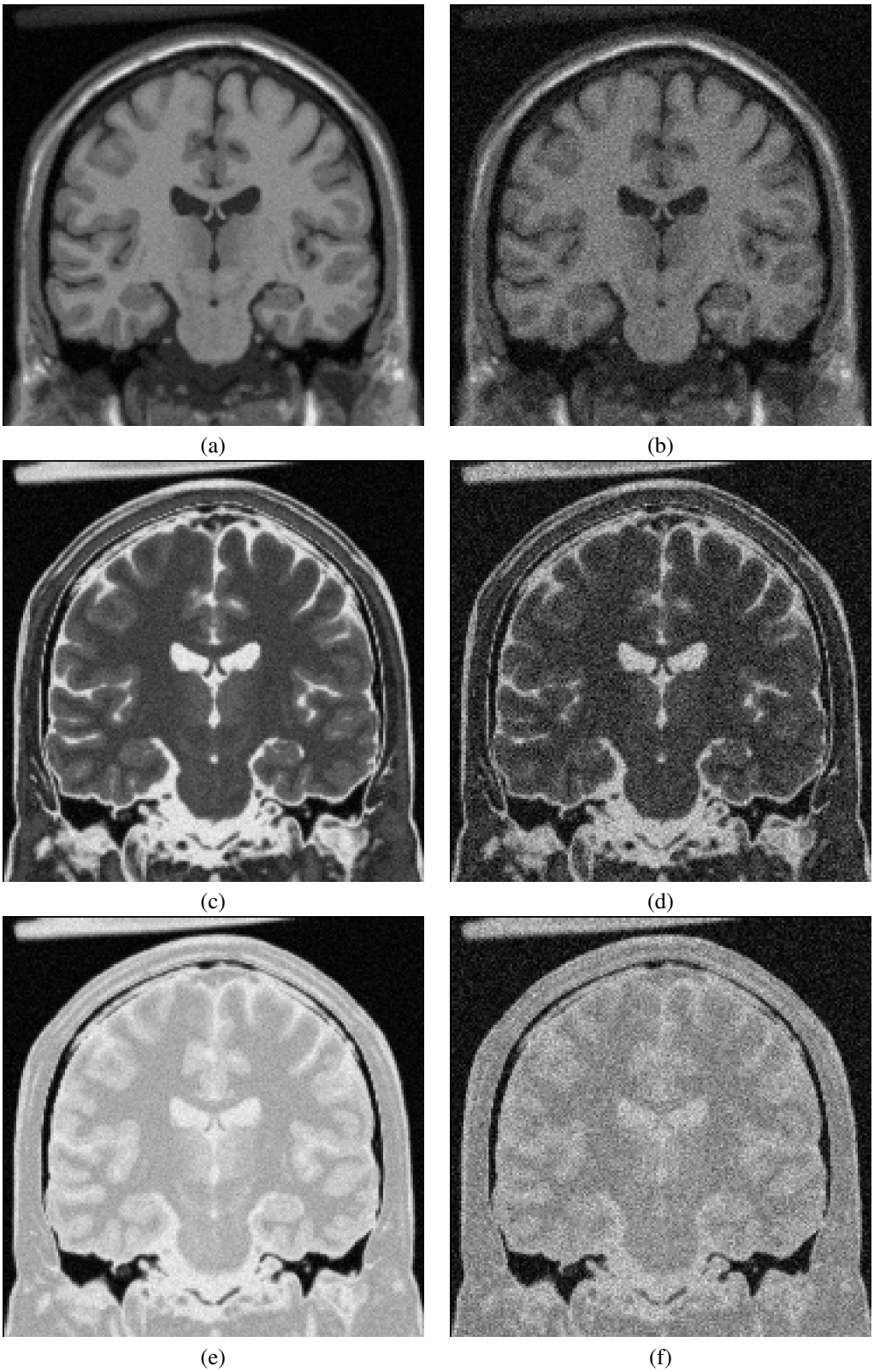

Fig. 5. Coronal slices of synthetic (a)-(b) T1; (c)-(d) T2; and (e)-(f) PD images. The slices in the left and right present high and low SNR, respectively.

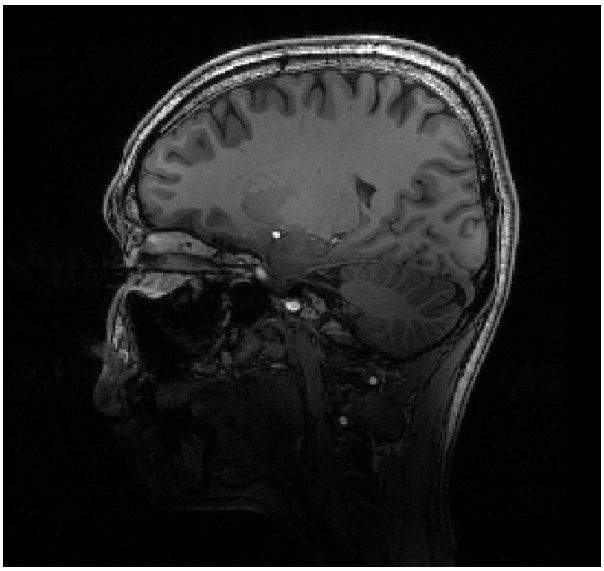

Fig. 6. Sagittal slice of T1-weighted image with high inhomogeneity effect. The intensity of the image is lower in the inferior part of the image.

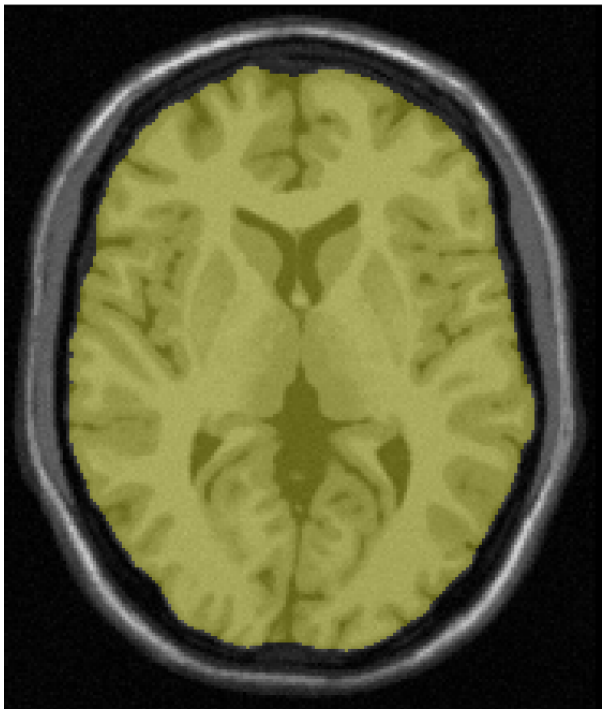

Fig. 7. Axial slice of T1-weighted image. The yellow label contains the brain after skull stripping.

There are several solutions that generate the corrected image in a direct or indirect way. The only solutions that only relly on the input image are the Non-parametric Non-uniform intensity Normalization (N3) [14] and N4ITK [65]. N3 is available in Freesurfer software suite [8] and N4ITK is available in 3D Slicer. For any non-brain MRI applications, these are the best solutions and are relatively easy to use, with few parameters. BrainSuite provides a method called BFC Correction Tool. It has an automatic and a semiautomatic solution in which the user selects GM, WM and CSF points for the inhomogeneity correction. Other software such as FSL and Statistical Parametric Mapping (SPM) [9], may output a corrected image after executing a more complex task, such as brain tissue segmentation, or brain registration and complete segmentation.

C. Intensity normalization

One last crucial operation for many applications that involve population studies is the intensity normalization or standardization. The objective is to have the voxels of corresponding tissues and organs in all images within a similar range of intensity. For that purpose, statistic moments of the image histogram may be used to adjust the complete range of intensities. A reference image is employed for the adjustment of all other images.

Study [19] concluded that intensity normalization prior to inhomogeneity correction improves significantly the post-processing results. One could use Freesurfer or Cavass [10] [66] for intensity standardization. Freesurfer executes standardization twice: before and after skull stripping. Cavass provides few parameter choices for a better configuration according to the application and may be used for any MR image, not just for the brain region.

[8]http://freesurfer.net/

[9]http://www.fil.ion.ucl.ac.uk/spm/

[10]http://www.mipg.upenn.edu/Vnews/mipg_software.html

IV. Segmentation

MRI segmentation is a very useful procedure for volume/size measurement, form estimation, and also as a prior step to other image operations. The strategies employed to segment MRI, already mentioned in Section I, vary from intensity based, gradient based, clustering, supervised classification, and model based methods among others. There is a distinct segmentation process for MRI time series, when there is a physiological motion of the scanned area, such as breathing or heart beating. In these cases, one may also use information based on intensity or border variation [67] [68].

Next, we will discuss the most important segmentation steps for brain image processing and analysis.

A. Skull stripping

Skull stripping is one of the first segmentation procedures for MRI of the brain. Image 7 shows an example of this operation. Unfortunately, there is no precise definition of what skull stripping operation is. According to previous works, brain extraction can be described as: “to isolate brain from extracranial or non-brain tissues” [69], “removing the skull and non-brain tissues” [70], and “whole-brain segmentation” [71]. These descriptions are oversimplified and little attention has been paid for some important details.

Skull stripping is required for inhomogeneity correction by most of the proposed methodologies, except for N3 and N4.

On the other hand, it has being proved that inhomogeneity correction may also influence skull stripping, specially for high magnetic field MRI acquisitions [72].

All the software mentioned in Section III can isolate the brain from skull and scalp. Nevertheless, some software such as SPM provide the mask of the brain while segmenting the tissues and registering the image to a standard space. This happens because the main objective of SPM is fMRI studies and not structural MRI research.

As mentioned before, the brain is composed by GM and WM tissues, surrounded by CSF. Structurally, the brain is divided into three main regions: the forebrain that contains the telencephalon, i.e. two cerebral hemispheres, and the diencephalon; the midbrain; and the hindbrain that includes the metencephalon and the myenlencephalon which contains the cerebellum.

The importance of CSF delineation depends on the purpose of brain extraction. It is fundamental for brain atrophy estimation [73] but irrelevant for functional analysis of subcortical structures of drug and alcohol dependent patients [74]. Because of the distinct expectations and because of the extra effort to segment external CSF, a few datasets like Brainweb Phantom [12] provide surrounding CSF in its ground-truth, while others such as the Internet Brain Segmentation Repository (IBSR) [11] only discriminate CSF inside the ventricles and disconsider external CSF. The majority of the ground-truths in T2-weighted MRI databases, on the other hand, include brain surrounding CSF since it is much easier to delineate [75].

B. Brain tissue segmentation and classification

Tissue segmentation is very important for studying degenerative pathologies and for planning surgeries. The output of this operation is illustrated in Figure 3, showing brain voxels labeled in three different tissues: WM, GM, and CSF.

A similar operation is called tissue classification. Instead of labeling each voxel as belonging to one tissue type, each voxel receives a probability of containing CSF, GM, WM or non-brain material, such as bone, eyes, background, etc. Classification takes into account that each voxel is large enough to have partial volume of more than one tissue type [76]. Some software such as FAST from FSL [21] provide a segmentation into a higher number of labels of the brain tissues, containing partial volume of GM+WM, CSF+GM, and CSF+background.

Depending on the final application, partial volume effect must be considered, specially when small subcortical regions are of greater interest. However, as we evaluate methods accuracy by means of the ground-truths, these solutions are not very effective. Brain tissue gold standards are almost impossible to be delineated manually or even semi-automatically because of the sulci and gyri irregular shape [77], [34]. Partial volume segmentation would multiply the amount of required work for a proper segmentation since humans are unable to define the exact proportion of GM, WM, and CSF contained in any voxel. Using automatically classified ground-truths is also not a good solution, since it will bias the results toward the type of the employed methodology. Synthetic datasets have been used as one of the best solutions [78]. None the less, they do not provide the same challenges as real images.

Other researchers [79], [80] propose to evaluate tissue segmentation without a ground-truth. The idea is to compare sereval methods among themselves. There are two problems with this approach: first, all methods must use very distinct methodologies, otherwise the result will be biased to benefit the class of similar methods that appears in greater number; second, one method that outperforms the others will be penalized by generating the unique best result.

C. Smaller structure segmentation

The segmentation of other cortical and subcortical structures are useful for more specific tasks. For instance, the thalamus is important for cocaine and alcohol addiction studies [81]. In [82] the thalamus was segmented in an efficient way using a clustering approach associating tissue intensity and probabilistic atlas information.

Generally, a more complex procedure is required in these cases compared to tissue segmentation and skull stripping, since the borders of brain structures may not be well defined. One must use an adaptive model such as the ones used to segment the hemispheres and the cerebellum in [83] or an atlas, as in SPM and Freesurfer.

The evaluation of brain structures, specially the small ones, are less challenging, since it is possible to segment them manually in a reasonable time and very accurately. One may use distance based or region based metrics for that purpose. We suggest paper [84] for a complete list of metrics for all kinds of segmentation.

Finally, brain tumor segmentation is among the most challenging procedures that involve MRI, since they have no clear pattern such as intensity, form, size or location. We recommend the readers to [85] for a complete review in this subject.

V. Pose and spatial standardization

A. Image interpolation

Image interpolation is used to improve many aspects of MR images. It is essential for a variety of medical imaging processing, such as, image generation, compression or resampling, subpixel translation, elastic deformation or warping, magnification or minification, and geometrical correction [86] [87] [88]. This process is required for image registration and proper volume visualization.

Image interpolation is a more consolidated issue and the most commonly used interpolation technique are: nearest neighbor, bilinear, bicubic, B-splines, lanczos2, discrete wavelet transform and Kriging [89].

B. Motion correction

MRI acquisition of a single 3D image takes several minutes. Meantime, the patient may move the head during a run or between runs, resulting in wrong spatial location. Therefore,

[11] http://www.nitrc.org/projects/ibsr/

some voxels might mix the signal of two different tissue types or may miss important information from the edges of a tissue. There are many accessories used to reduce the movement of the head, such as, padding, bite bar, vacuum cushion or face mask, but it is impossible to avoid movements as small as a few millimeters. As MRI resolution is millimetric, small movements will dishevel or distort the image sequence.

The motion correction should be carried out co-registering each volume in the sequence run acquisition to a reference volume. The possible reference volume may be: i) First volume in the sequence acquisition; ii) Middle volume in the sequence acquisition; or iii) Average of all the volumes in the sequence acquisition prior to motion correction. It should be said that there is no consensus about which reference volume is the best, but typically first acquired volume is used for motion correction.

C. Image registration

Prior to image registration and to other processes such as skull stripping, it may be important to estimate the pose of the image. That is, to detect the overall position and orientation that the scanned body is. There is a distinct methodology for each body part. For brain MRI, we recommend the reader to [90].

In general, image registration is defined as the search for a geometrical transformation that aligns corresponding points of an object in two or more different images. Computerized methods provide accurate alignment of the information contained in different images and allow the visualization of the combined images. The spatial transformation of an image data set to a common reference domain will help the researcher to: i) communicate and compare data (across subjects, time, conditions, and image types); ii) classify data (by meaningful spatial positions or extent); and iii) find patterns in data (to infer structural or functional relationships) [91] [92].

Image registration methods are taken under these two different conditions: images from different instants of time from the same subject (intra-subject registration) and the registration of images from two or more individuals (inter-subject registration). Inter-subject brain image registration is the most challenging one because distinct brains vary in shape and size. Even the registration of the same brain over time is far from perfect [91]. Manual labeling is not very reliable [77] and becomes prohibitive in terms of time and resource when several brain images are processed [92].

The operational of image registration aligns a "registered" image to a target domain, which may be another image or a reference coordinate system, such as a template atlas. The Original Talairach & Tournoux is an atlas based on one postmortem brain, and MNI152 was generated based on the average position of a group of images.

There are many image registration methods categorized in linear and non-linear approaches [93] [94]. Rigid body is a linear transformation that aligns 3D images using 6 degree of freedom (DOF), composed of 3 rotations and 3 translations; and it is used for intra-subject registration when there is no image distortion. Affine is also a linear transformation which uses 12 DOF, composed of 3 rotation, 3 translations, 3 stretches and 3 shears; it is used for intra-subject registration when there is global gross-overall distortion, eddy current correction. It is also very commonly used prior to non-linear registration. Non-linear transformation is used for a robust inter-subject registration and image distortion correction. Many different parametrization can be used, such as, General diffeomorphisms (e.g. fluid models), Spline parametrization (b-splines, thin-plate splines), and Fourier parametrization.

1) **Popular techniques.** Popular software used for image registration are: FSL [93], SPM; Freesurfer, Advanced Normalization Tools (ANTs) [12] [95], [96], and elastix [13] [97]. Besides these software there are many other algorithms elsewhere [92].
   For linear and non-linear image registrations FLIRT and FNIRT from FSL [93], respectively, are open-source software. FLIRT uses MNI152 template on standard mode. FNIRT allows local deformations by a linear followed by a non-linear method [92].
   SPM is a Matlab toolbox, and it offers different registration algorithms: traditional deformable normalization, Unified Segmentation, and DARTEL.
   Freesurfer is Linux open-source brain image analysis library with many different registration tools, each one designed for specific purposes. As FSL, this package is easy to install and runs in a command line interface.
   Elastix and ANTs may be used not only for brain image registration but also for other body parts. They are also easy to install and multi-plataform.
2) **Evaluation process.** During the process of image registration, an optimization algorithm iteratively adjusts the values of DOF to estimate the best matching parameters. Optimal registration is found when an extreme value of cost function is found.
   The evaluation process that measures the quality of the match is based on a minimization or maximization cost function. Many different cost function have been proposed for optimizing image registration. Recent registration methods have used intensitybased cost functions [98] that are more accurate and reliable than the geometric-based [99]. Intensity-based cost function can be grouped in two category: these suitable for intra-subject analysis and these for inter-subject analysis. For intra-subject analysis the most common cost functions are: least square and normalized correlation. For inter-subjects category, the most used are: mutual information, normalized mutual information woods and correlation ratio [98] [100].

VI. Acquisition and processing of fMRI

This and the following sections are extracted from [101], in which additional details are available.

[12] http://stnava.github.io/ANTs
[13] http://elastix.isi.uu.nl

A. Acquisition

FMRI provides an indirect measure of brain activity by means of a blood-oxygenation-level dependent contrast or BOLD signal in short, as discovered by Ogawa and colleagues [102]. The BOLD signal measures changes in the amount of deoxygenated hemoglobin, resulting from a larger consumption of oxygen when neurons are activated, and increased blood flow and volume. Active neurons generate an increase in the amount of deoxygenated hemoglobin, leading to brighter MR images or an increase in BOLD signal. The term BOLD hemodynamic response (HR) is commonly used to refer to the shape of the BOLD signal following a neuronal event, and could be conceptualized as the impulse response of BOLD. The hemodynamic response shows its peak in 6s and an undershoot around 10s after the stimulus is presented, as a result of the changing dynamics of cerebral blood flow and volume. It must be noted that the hemodynamic response will vary depending on the duration and number of the environmental stimuli driving neuronal responses. Complex image acquisition and reconstruction processes are involved to turn BOLD signals into 3D images. An excellent introduction and review of fMRI is available in Huettel et al. [103].

In terms of image acquisition, two main components apply to fMRI data:

Spatial resolution: the ability to distinguish signal differences between nearby spatial locations. In fMRI, images are often obtained in 64×64 or 256×256 matrix (referred as slice). For a field of view of 220 by 220 mm and a matrix of 64×64, the in-plane voxel size would be 3.44 by 3.44 mm. The third dimension is generally the same as or larger than the in-plane voxel size, and depends on how many slices one might want to obtain for one particular study.

Temporal resolution: the ability to distinguish signal differences between sequential observations. Temporal resolution is given by the repetition time (TR). TR is usually between 500ms and 3s, and is the time necessary for the scan to resample from the same voxel. One of the MR scanner parameters related to temporal resolution is the flip angle, which is the change in net longitudinal magnetization after excitation pulse. The shorter the TR is, the smaller the flip angle has to be. Thus, smaller TR means higher temporal resolution, but it also means decreased BOLD signal and reduced spatial coverage, because of the reduced flip angle.

B. Preprocessing

After fMRI acquisition and reconstruction, there are a series of computational procedures to correct for unwanted variability (noise) and artifacts, and to prepare the images for further statistical analysis. These procedures are known as preprocessing in the fMRI literature and similar regardless of the experimental design and the purpose of statistical analyses. The most common preprocessing steps in fMRI are:

1) Realignment: corrects for misalignment of the images across the slices and scan sessions, originating basically from the head movement. Assuming the head as a solid, rigid-body transformations (rotation and translation) are applied, based on some image similarity measures.
2) Slice-timing correction: when associating each slice (in-plane image) with a time point, it must be noted that there is a time delay from the start to the end of scanning of each single slice. This phase delay must be corrected, using some interpolation technique.
3) Unwarping: corrects for distortions in the images, generated by inhomogeneities in the magnetic field. In addition to the machines imprecision, head size and location are sufficient to create inhomogeneity or bias field.
4) Spatial normalization: registers different subjects brains to a common stereotaxic space, such as Talairach space and Montreal Neurological Institute (MNI) space. Normalization is necessary when comparing subjects BOLD signals in a group. Normalization also allows the localization of a particular brain structure of interest through an anatomical atlas.
5) Smoothing: a spatial filtering is performed by means of a Gaussian kernel to reduce noise and enhance the statistical power for group comparisons. This also has to do with the imprecise nature of the spatial normalization process.

These preprocessing methods are available in popular softwares such as SPM and FSL.

VII. Statistical analyses

The first component to be considered in a fMRI study is the experimental design, which depends on the brain function to be investigated and the question to be answered. Further, different statistical and computational methods can be used to delineate brain regions that are activated or functionally connected during the realization of a particular event or function.

A. Experimental design

We can classify the fMRI experiments into three classes:

Block design: the stimuli are presented in a multiple, consecutive way or constantly, and divided into different experimental conditions. For example, a visual stimulus can be presented in one block, and a constant bip sound can be presented in another condition, forming two distinct conditions. One can thus differentiate the BOLD signal level across conditions, and localize the brain activations specific to each of the two conditions, using standard statistical methods.

Event-related design: the stimuli are presented in short and discrete intervals, each constituting a single event or trial. A fMRI session is formed by a sequence of stimuli/events, constituting different conditions depending on a particular set of stimuli. The duration between two consecutive events is known as inter-stimulus interval (ISI).

Resting-state experiment: there are no stimuli and the aim is to collect the brain's BOLD signal during a resting state, and investigate the brain's underlying activity when no external stimulus is presented. Resting state BOLD data have been instrumental in defining clusters of brain regions

that are functionally connected including the default-mode network [104].

Because resting-state fMRI is straightforward to run and easy to compare across different investigations, it became one of the most popular approaches in functional brain connectivity analysis [105]. On the other hand, block and event-related designs are required to investigate condition-specific functional connectivity, common during cognitive challenges.

B. Activation maps

Traditionally, brain activation maps are obtained using the block and event-related designs. Employing a mass-univariate approach, experimental conditions are entered in a general linear model (GLM), and a statistical parametric map is obtained. In the GLM, the BOLD signal is the explained variable, and the conditions/events are the regressors. The event regressors are convolved by a hemodynamic response (HR) function to account for the delay of the BOLD signal. All the relevant conditions must be entered in the design matrix of the GLM to acount for the BOLD variability. For instance, usually the head movement parameters as well as physiological variables, when available, are entered as covariates of no interest. The GLM estimates the component of variance explained by each of the regressors, with the coefficient of each regressor constituting a β image. The β image reflects the height of average activation across trials for a particular event. Further, these β images are contrasted in order to ascertain that a particular brain region is more active during condition A than B (baseline condition). Finally, for each individual and experimental condition, a contrast con image is obtained. Often, this step is called *first-level analysis*.

The con images can be used to perform one-sample t-tests and obtain individual activation maps. However, these maps are very variable across individuals and are not representative of the group. Therefore, in a so called *second-level* or *group analysis*, the contrast images (con) of the first-level analyses are used for random-effect analysis to obtain group T-maps, such as one-sample t tests. Alternatively, the con images can be used in other parametric tests, two-sample t tests, analysis of variance (Anova), etc.

C. Functional connectivity

Investigation of the functional connectivities between brain regions is critical to our understanding of how information is integrated in the brain [106]. The functional methods can be divided in three classes:

Seed-based methods: a single ROI is selected, an average or representative time-series is extracted for a region of interest (ROI), and a functional connectivity measure is computed for every pair ROI-to-voxel across the whole-brain. Thus, these are bivariate approaches, and sometimes referred to as whole-brain methods. In this category, we have the correlation analysis of resting-state data [107], bivariate Granger causality [108] and psychophysiological interaction or PPI [109].

ROI-based methods: multiple ROIs are selected from a previous functional localization analysis of the fMRI data (activation maps); i.e., parts of the brain that are active during a condition of interest; or from an anatomical atlas of the brain. A connectivity hypothesis is tested based on the network obtained from the time-series modeling of these ROIs. In this category, we have techniques based on structural equation modeling or SEM [110], multivariate Granger causality [111], and dynamic causal modeling or DCM [112].

Data-driven approach: connected regions are selected in a completely data-driven fashion. Multiple time-series are classified into groups or clusters according to some criterion, such as independent component analysis (ICA) [113], in which clusters are formed based on the spatio temporal characteristics of the BOLD signal of every single voxel.

Although these approaches are here classified separately, they are complementary and usually employed in conjunction. For instance, ICA can be used to select networks of interest, which in turn are used as the ROIs of the multivariate Granger causality [114]. PPI analysis is used to localize regions connected to a particular ROI, followed by a multivariate Granger causality analysis [115].

D. Traps and pitfalls

In this subsection we summarize some of the concerns that previous studies have raised when performing statistical analysis on fMRI data [116], [117], [118] and point out possible directions to resolve these issues.

Imaging artifacts: BOLD signals suffer from several artifacts: distortion, partial volume effects, large vessel effects [103]. Thus, before performing fMRI data analyses, one must pay attention to the quality of preprocessed output images. A visual quality check of the preprocessed fMRI data is always recommended. A good material for image quality check is available in PhysIO Toolbox, part of the TAPAS software[14].

Imperfect normalization: despite the availability of very accurate normalization algorithms, no alignment between subjects brains can be perfect because of the inter-subject variability in brain anatomy. For example, for functional connectivity analysis, one should be aware of this inaccuracy when extracting the average BOLD time-series from a particular anatomical atlas. This might have direct impact on the functional connectivity results, because the latter is affected by anatomically inaccurate ROIs, as observed by [116]. Functionally parcelled atlas is suggested to ameliorate the anatomical inaccuracy.

Hemodynamic response (HR) variability: it has long been known that different regions in the brain has different HR [119], and this poses a critical concern to the lag-based connectivity methods, since they take the temporal precedence as granted to infer connectivity. In particular, recent investigations have shown poor performance of these lag-based methods in connectivity modeling [116]. Deconvolution methods are suggested for a more accurate modeling of the HR functions [120].

[14] https://www.tnu.ethz.ch/de/software/tapas.html).

VIII. fMRI PATTERN ANALYSIS

In the past decade, the use of pattern recognition tools became popular in fMRI data analysis, and they are used to complement traditional statistical methods. A nice review of the progress of fMRI analyses within the field of neuroscience can be found in [121].

A. Encoding pattern analysis

As we saw in the previous section, traditional fMRI statistical methods such as the GLM requires a priori task-design and is limited to observable or at least measurable task conditions (regressors). These methods can be understood as encoding analyses, in which the parameters of a priori defined model are estimated given the BOLD signal for each single voxel. In other words, the BOLD signal of a single voxel is mapped to many experimental conditions. In this approach, there is no consideration of interdependencies between multiple voxels. To perform encoding analyses (GLMs), readers are directed to use packages such as SPM and FSL.

B. Decoding pattern analysis

Modern fMRI analysis methods are based on pattern recognition techniques, and aim to map multiple voxels (BOLD signals) to a single experimental condition. These approaches are called decoding or mind-reading techniques[122]. An example would be to use SVM to map a set of BOLD signals to an experimental condition, in a single time point. To perform fMRI decoding, popular softwares using Matlab such as Pronto [123] are avaible[15].

C. Multi-voxel pattern analysis

An extension of the decoding methods would be the multi-voxel pattern analysis or MVPA [47], [124]. In this approach, a many-to-many mapping (voxels to experimental conditions) is performed. This would be a generalization of the two previous approaches. Nice softwares are avaialable in Matlab and Python such as Princeton MVPA toolbox[16] and the PyMVPA[17].

In addition to these single subject approaches (encoding or decoding of mental states), pattern recognition tools can be used to classify individuals into different groups. An introductory review can be found in [125]. One can use single classifiers like in Pronto or combine different classifiers using fusion methods [126].

IX. SHORT BIOGRAPHY

Fábio Augusto Menocci Cappabianco is Bachelor of in Computer Engineering from University of Campinas in 2003, M.Sc. in Computer Science from University of Campinas in 2006 (dissertation in computer architectures for image processing, supervisor Guido Araujo), and got his doctorate in Computer Science from University of Campinas and University of Pennsylvania in 2010 (thesis in MRI of the brain, supervisors Alexandre Falcão and Jayaram Udupa). He is currently as assistant professor at the Federal University of São Paulo, teaching graduate courses in Computer Science and Biomedical Engineering. He has experience in the area of image processing, with emphasis on biomedical imaging and computer architecture.

Claudio Saburo Shida received B.Sc. in Physics from University of São Paulo in 1990, M.Sc. in Physics from University of São Paulo in 1993, and he got his doctorate in Physics from University of São Paulo (1998). Claudio is post doctorate from Daresbury Laboratory, England in 1999, from University of São Paulo in 2002, and from Federal University of Rio de Janeiro in 2014. He is currently as assistant professor at the Federal University of São Paulo.

Jaime Shinsuke Ide is Assistant Director at LCNeuro and Research Assistant Professor in the Department of Biomedical Engineering at Stony Brook University. Prior, he was Assistant Professor at Federal University of São Paulo. He is Bachelor of Mechatronic Engineering, and Ph.D. in Engineering (dissertation focused in Probabilistic Graphical Models and Computational Statistics, supervisor Professor Fabio G. Cozman) from University of São Paulo. He received training in MRI in the Department of Radiology at University of Pennsylvania (2007-2008), and worked with Bayesian methods for brain-image segmentation and registration. Further, he received training in fMRI at Yale University (2008-2010), under supervision of Professor Chiang-shan Ray Li, MD., PhD. in exciting projects including investigations of functional connectivity of brain areas involved in cognitive control.

[15]http://www.mlnl.cs.ucl.ac.uk/pronto/

[16]https://pni.princeton.edu/pni-software-tools/mvpa-toolbox

[17]http://www.pymvpa.org/

ACKNOWLEDGMENT

The authors would like to thank CNPq (486988/2013-9) and FAPESP (14/12559-5) for financial supports.

REFERENCES

[1] D. A. Dewsbury, "The 1973 nobel prize for physiology or medicine: recognition for behavioral science?" *American Psychologist*, vol. 58, no. 9, p. 747, 2003.

[2] F. W. Wehrli, "On the 2003 nobel prize in medicine or physiology awarded to paul c. lauterbur and sir peter mansfield," *Magnetic Resonance in Medicine*, vol. 51, no. 1, pp. 1–3, 2004.

[3] C. Jack, R. Petersen, P. O'Brien, and E. Tangalos, "MR-based hippocampal volumetry in the diagnosis of Alzheimer's disease," *Neurology*, vol. 42, no. 1, pp. 183–188, 1992.

[4] A. Bastos, R. Comeau, F. Andermann, D. Melanson, F. Cendes, F. Dubeau, S. Fontaine, D. Tampieri, and A. Olivier, "Diagnosis of subtle focal dysplastic lesions: Curvilinear reformatting from three-dimensional magnetic resonance imaging," *Annals of Neurology*, vol. 46, no. 1, pp. 88–94, 1999.

[5] M. Filippi, M. A. Rocca, O. Ciccarelli, N. De Stefano, N. Evangelou, L. Kappos, A. Rovira, J. Sastre-Garriga, M. Tintorè, J. L. Frederiksen *et al.*, "Mri criteria for the diagnosis of multiple sclerosis: Magnims consensus guidelines," *The Lancet Neurology*, vol. 15, no. 3, pp. 292–303, 2016.

[6] M. Kushnirsky, V. Nguyen, J. S. Katz, J. Steinklein, L. Rosen, C. Warshall, M. Schulder, and J. P. Knisely, "Time-delayed contrast-enhanced mri improves detection of brain metastases and apparent treatment volumes," *Journal of neurosurgery*, pp. 1–7, 2015.

[7] R. A. Bermel and R. T. Naismith, "Using mri to make informed clinical decisions in multiple sclerosis care," *Current opinion in neurology*, vol. 28, no. 3, pp. 244–249, 2015.

[8] G. S. Dichter, D. Gibbs, and M. J. Smoski, "A systematic review of relations between resting-state functional-mri and treatment response in major depressive disorder," *Journal of affective disorders*, vol. 172, pp. 8–17, 2015.

[9] J. Van Waarde, H. Scholte, L. van Oudheusden, B. Verwey, D. Denys, and G. van Wingen, "A functional mri marker may predict the outcome of electroconvulsive therapy in severe and treatment-resistant depression," *Molecular psychiatry*, vol. 20, no. 5, pp. 609–614, 2015.

[10] J. S. Ide, S. Hu, S. Zhang, L. R. Mujica-Parodi, and C. shan R. Li, "Power spectrum scale invariance as a neural marker of cocaine misuse and altered cognitive control," *NeuroImage: Clinical*, vol. 11, pp. 349 – 356, 2016.

[11] S. W. Atlas, *Magnetic resonance imaging of the brain and spine*. Lippincott Williams & Wilkins, 2009, vol. 1.

[12] C. A. Cocosco, V. Kollokian, R. K.-S. Kwan, G. B. Pike, and A. C. Evans, "Brainweb: Online interface to a 3d mri simulated brain database," in *NeuroImage*. Citeseer, 1997.

[13] K. Uludağ, K. Uğurbil, and L. Berliner, *fMRI: From Nuclear Spins to Brain Functions*. Springer, 2015, vol. 30.

[14] J. G. Sled, A. P. Zijdenbos, and A. C. Evans, "A nonparametric method for automatic correction of intensity nonuniformity in MRI data," *IEEE Transactions on Medical Imaging*, vol. 17, no. 1, pp. 87–97, 1998.

[15] L. Q. Zhou, Y. M. Zhu, C. Bergot, A. M. Laval-Jeantet, V. Bousson, J. D. Laredo, and M. Laval-Jeantet, "A method of radio-frequency inhomogeneity correction for brain tissue segmentation in MRI," *Computerized Medical Imaging and Graphics*, vol. 25, no. 5, p. 379, 2001.

[16] E. B. Lewis and N. C. Fox, "Correction of differential intensity inhomogeneity in longitudinal MR images," *Neuroimage*, vol. 23, no. 1, pp. 75–83, 2004.

[17] A. M. Dale, B. Fischl, and M. I. Sereno, "Cortical surface-based analysis: I. Segmentation and surface reconstruction," *Neuroimage*, vol. 9, no. 2, pp. 179–194, 1999.

[18] D. W. Shattuck, S. R. Sandor-Leahy, K. A. Schaper, D. A. Rottenberg, and R. M. Leahy, "Magnetic resonance image tissue classification using a partial volume model," *NeuroImage*, vol. 13, no. 5, pp. 856–876, 2001.

[19] A. Madabhushi, J. K. Udupa, and A. Souza, "Generalized scale: Theory, algorithms, and application to image inhomogeneity correction," *Computer vision and image understanding*, vol. 101, no. 2, pp. 100–121, 2006.

[20] J. Milles, Y. M. Zhu, G. Gimenez, C. R. G. Guttmann, and I. E. Magnin, "MRI intensity nonuniformity correction using simultaneously spatial and gray-level histogram information," *Computerized Medical Imaging and Graphics*, vol. 31, no. 2, pp. 81–90, 2007.

[21] Y. Zhang, M. Brady, and S. Smith, "Segmentation of brain MR images through a hidden markov random field model and the expectation-maximization algorithm," *IEEE Transactions on Medical Imaging*, vol. 20, no. 1, pp. 45–57, 2001.

[22] M. N. Ahmed, S. M. Yamany, N. Mohamed, A. A. Farag, and T. Moriarty, "A modified fuzzy c-means algorithm for bias field estimation and segmentation of MRI data," *IEEE Transactions on Medical Imaging*, vol. 21, no. 3, pp. 193–199, 2002.

[23] R. Bansal, L. H. Staib, and B. S. Peterson, "Correcting nonuniformities in MRI intensities using entropy minimization based on an elastic model," in *Medical Image Computing and Computer-Assisted Intervention*. Springer, 2004, pp. 78–86.

[24] E. G. Learned-Miller and P. Ahammad, "Joint MRI bias removal using entropy minimization across images," in *Neural Information Processing Systems*, vol. 17, 2005, pp. 761–768.

[25] U. Vovk, F. Pernuš, and B. Likar, "Intensity inhomogeneity correction of multispectral MR images," *Neuroimage*, vol. 32, no. 1, pp. 54–61, 2006.

[26] C. Lee, S. Huh, T. A. Ketter, and M. Unser, "Unsupervised connectivity-based thresholding segmentation of midsagittal brain MR images," *Computers in Biology and Medicine*, vol. 28, no. 3, pp. 309–338, 1998.

[27] V. Grau, A. U. J. Mewes, M. Alcaniz, R. Kikinis, and S. K. Warfield, "Improved watershed transform for medical image segmentation using prior information," *IEEE Transactions on Medical Imaging*, vol. 23, no. 4, pp. 447–458, 2004.

[28] S. K. Warfield, M. Kaus, F. A. Jolesz, and R. Kikinis, "Adaptive, template moderated, spatially varying statistical classification," *Medical Image Analysis*, vol. 4, no. 1, pp. 43–55, 2000.

[29] W. M. Wells III, W. E. L. Grimson, R. Kikinis, and F. A. Jolesz, "Adaptive segmentation of MRI data," *IEEE Transactions on Medical Imaging*, vol. 15, no. 4, pp. 429–442, 1996.

[30] Z. Song, S. P. Awate, and J. C. Gee, "Nonparametric Markov priors for tissue segmentation," in *IEEE ISBI*, 2008, pp. 73–76.

[31] C. A. Cocosco, A. P. Zijdenbos, and A. C. Evans, "A fully automatic and robust brain MRI tissue classification method," *Medical Image Analysis*, vol. 7, no. 4, pp. 513–527, 2003.

[32] J. Sijbers, P. Scheunders, M. Verhoye, A. Van der Linden, D. Van Dyck, and E. Raman, "Watershed-based segmentation of 3D MR data for volume quantization," *Journal of Magnetic Resonance Imaging*, vol. 15, no. 6, pp. 679–688, 1997.

[33] K. Van Leemput, F. Maes, D. Vandermeulen, and P. Suetens, "Automated model-based tissue classification of MR images of the brain," *IEEE Transactions on Medical Imaging*, vol. 18, no. 10, pp. 897–908, 1999.

[34] A. P. Zijdenbos, R. Forghani, and A. C. Evans, "Automatic "pipeline" analysis of 3-D MRI data for clinical trials: Application to multiple sclerosis," *IEEE Transactions on Medical Imaging*, vol. 21, no. 10, pp. 1280–1291, 2002.

[35] J. Yang, L. H. Staib, and J. S. Duncan, "Neighbor-constrained segmentation with level set based 3-D deformable models," *IEEE Transactions on Medical Imaging*, vol. 23, no. 8, pp. 940–948, 2004.

[36] K. M. Pohl, J. Fisher, R. Kikinis, W. E. L. Grimson, and W. M. Wells, "Shape based segmentation of anatomical structures in magnetic resonance images," *Computer Vision for Biomedical Image Applications*, vol. 3765, pp. 489–498, 2005.

[37] M. Prastawa, J. H. Gilmore, W. Lin, and G. Gerig, "Automatic segmentation of MR images of the developing newborn brain," *Medical Image Analysis*, vol. 9, no. 5, pp. 457–66, 2005.

[38] S. P. Awate, T. Tasdizen, N. Foster, and R. T. Whitaker, "Adaptive Markov modeling for mutual-information-based, unsupervised MRI brain-tissue classification," *Medical Image Analysis*, vol. 10, no. 5, pp. 726–39, 2006.

[39] U. Yoon, V. S. Fonov, D. Perusse, and A. C. Evans, "The effect of template choice on morphometric analysis of pediatric brain data," *Neuroimage*, vol. 45, no. 3, pp. 769–777, 2009.

[40] K. Nakamura and E. Fisher, "Segmentation of brain magnetic resonance images for measurement of gray matter atrophy in multiple sclerosis patients," *Neuroimage*, vol. 44, no. 3, pp. 769–776, 2009.

[41] P. Teo, G. Sapiro, and B. Wandell, "Creating connected representations of cortical gray matter forfunctional MRI visualization," *Medical Imaging, IEEE Transactions on*, vol. 16, no. 6, pp. 852–863, 1997.

[42] F. Cappabianco, A. Falcão, C. Yasuda, and J. Udupa, "Brain tissue MR-image segmentation via optimum-path forest clustering," *Computer Vision and Image Understanding*, 2012.

[43] G. Aguirre, J. Detre, E. Zarahn, and D. Alsop, "Experimental design and the relative sensitivity of bold and perfusion fmri," *Neuroimage*, vol. 15, no. 3, pp. 488–500, 2002.

[44] K. J. Worsley and K. J. Friston, "Analysis of fmri time-series revisitedagain," *Neuroimage*, vol. 2, no. 3, pp. 173–181, 1995.

[45] K. J. Friston, A. P. Holmes, K. J. Worsley, J. P. Poline, C. D. Frith, and R. S. J. Frackowiak, "Statistical parametric maps in functional imaging: A general linear approach," *Human Brain Mapping*, vol. 2, no. 4, pp. 189–210, 1995.

[46] K. A. Norman, S. M. Polyn, G. J. Detre, and J. V. Haxby, "Beyond mind-reading: multi-voxel pattern analysis of fmri data," *Trends in cognitive sciences*, vol. 10, no. 9, pp. 424–430, 2006.

[47] J. V. Haxby, A. C. Connolly, and J. S. Guntupalli, "Decoding neural representational spaces using multivariate pattern analysis," *Annual review of neuroscience*, vol. 37, pp. 435–456, 2014.

[48] K. J. Friston, "Modalities, modes, and models in functional neuroimaging," *Science*, vol. 326, no. 5951, pp. 399–403, 2009.

[49] F. Bloch, "Nuclear induction," *Physical Review*, vol. 70, pp. 460–474, 1946.

[50] E. Purcell, H. Torrey, and R. Pound, "Resonance absorption by nuclear magnetic moments in a solid," *Physical Review*, vol. 69, pp. 37–38, 1946.

[51] P. C. LAUTERBUR, "Image formation by induced local interactions: Examples employing nuclear magnetic resonance," *Nature*, vol. 242, pp. 190–191, 1973.

[52] P. of MRI: A Primer, "Plewes, donald b. and kucharczyk, walter," *Journal of Magnetic Resonance Imaging*, vol. 35, p. 10381054, 2012.

[53] U. M. basic MR physics for physicians, "Currie, stuart and hoggard, nigel and craven,ian j. and hadjivassiliou, marios and wilkinson, iain d." *Postgrad Medical Journal*, vol. 89, p. 209223, 2013.

[54] A. Madabhushi and J. K. Udupa, "Interplay between intensity standardization and inhomogeneity correction in MR image processing," *IEEE Transactions on Medical Imaging*, vol. 24, no. 5, pp. 561–576, 2005.

[55] J. B. Johnson, "Thermal Agitation of Electricity in Conductors," *Phys. Rev.*, vol. 32, pp. 97–109, Jul 1928.

[56] H. Nyquist, "Thermal agitation of electric charge in conductors," *Phys. Rev.*, vol. 32, pp. 110–113, Jul 1928.

[57] S. M. Smith and J. M. Brady, "Susana new approach to low level image processing," *International journal of computer vision*, vol. 23, no. 1, pp. 45–78, 1997.

[58] G. Gerig, O. Kubler, R. Kikinis, and F. A. Jolesz, "Nonlinear anisotropic filtering of mri data," *IEEE Transactions on medical imaging*, vol. 11, no. 2, pp. 221–232, 1992.

[59] A. Fedorov, R. Beichel, J. Kalpathy-Cramer, J. Finet, J.-C. Fillion-Robin, S. Pujol, C. Bauer, D. Jennings, F. Fennessy, M. Sonka *et al.*, "3d slicer as an image computing platform for the quantitative imaging network," *Magnetic resonance imaging*, vol. 30, no. 9, pp. 1323–1341, 2012.

[60] J. V. Manjón, J. Carbonell-Caballero, J. J. Lull, G. García-Martí, L. Martí-Bonmatí, and M. Robles, "Mri denoising using non-local means," *Medical image analysis*, vol. 12, no. 4, pp. 514–523, 2008.

[61] X. Zhang, G. Hou, J. Ma, W. Yang, B. Lin, Y. Xu, W. Chen, and Y. Feng, "Denoising mr images using non-local means filter with combined patch and pixel similarity," *PloS one*, vol. 9, no. 6, p. e100240, 2014.

[62] A. Buades, B. Coll, and J.-M. Morel, "A non-local algorithm for image denoising," in *2005 IEEE Computer Society Conference on Computer Vision and Pattern Recognition (CVPR'05)*, vol. 2. IEEE, 2005, pp. 60–65.

[63] U. Vovk, F. Pernus, and B. Likar, "A review of methods for correction of intensity inhomogeneity in MRI," *IEEE Transactions on Medical Imaging*, vol. 26, no. 3, pp. 405–421, 2007.

[64] Cappabianco, Fábio and Miranda, Lellis, Lucas Santana and Miranda, Paulo Andre Vechiatto and Ide, Jaime Shinsuke and Mujica-Parodi, Lilianne, "Edge Detection Robust to Intensity Inhomogeneity: A 7T MRI Case Study," *The 21st IberoAmerican Congress on Pattern Recognition*, 2016, (to appear).

[65] N. J. Tustison, B. B. Avants, P. A. Cook, Y. Zheng, A. Egan, P. A. Yushkevich, and J. C. Gee, "N4itk: improved n3 bias correction," *IEEE transactions on medical imaging*, vol. 29, no. 6, pp. 1310–1320, 2010.

[66] G. Grevera, J. Udupa, D. Odhner, Y. Zhuge, A. Souza, T. Iwanaga, and S. Mishra, "Cavass: A computer-assisted visualization and analysis software system," *Journal of digital imaging*, vol. 20, no. 1, pp. 101–118, 2007.

[67] A. Pednekar, U. Kurkure, R. Muthupillai, S. Flamm, and I. A. Kakadiaris, "Automated left ventricular segmentation in cardiac mri," *IEEE Transactions on Biomedical Engineering*, vol. 53, no. 7, pp. 1425–1428, 2006.

[68] Cappabianco, Fábio and Tsuzuki, Marcos and Miranda, Paulo and Takimoto, Rogerio and Ueda, Edson and Sato, André and Rosset, Luciano and Rosso, Roberto Jr. and Gotoh, Toshiyuki and Iwasawa, Tae, "Determinao Automática da Caixa Contendo o Coraćão em Sequência Temporal de RM," *Congresso Brasileiro de Engenharia Biomdica*, 2016, (to appear).

[69] C. Fennema-Notestine, I. B. Ozyurt, C. P. Clark, S. Morris, A. Bischoff-Grethe, M. W. Bondi, T. L. Jernigan, B. Fischl, F. Segonne, D. W. Shattuck, R. M. Leahy, D. E. Rex, A. W. Toga, K. H. Zou, M. BIRN, and G. G. Brown, "Quantitative evaluation of automated skull-stripping methods applied to contemporary and legacy images: Effects of diagnosis, bias correction, and slice location," *Human brain mapping*, vol. 27, no. 2, pp. 99–113, 2006.

[70] L. A. Dade, F. Q. Gao, N. Kovacevic, P. Roy, C. Rockel, C. M. O'Toole, N. J. Lobaugh, A. Feinstein, B. Levine, and S. Black, "Semiautomatic brain region extraction: a method of parcellating brain regions from structural magnetic resonance images," *Neuroimage*, vol. 22, no. 4, pp. 1492–1502, 2004.

[71] F. Segonne, A. M. Dale, E. Busa, M. Glessner, D. Salat, H. K. Hahn, and B. Fischl, "A hybrid approach to the skull stripping problem in MRI," *Neuroimage*, vol. 22, no. 3, pp. 1060–1075, 2004.

[72] F. A. Cappabianco, P. A. de Miranda, J. S. Ide, C. L. Yasuda, and A. X. Falcao, "Unraveling the compromise between skull stripping and inhomogeneity correction in 3t mr images," in *2012 25th SIBGRAPI Conference on Graphics, Patterns and Images*. IEEE, 2012, pp. 1–8.

[73] N. C. Fox and P. A. Freeborough, "Brain atrophy progression measured from registered serial mri: validation and application to alzheimer's disease," *Journal of Magnetic Resonance Imaging*, vol. 7, no. 6, pp. 1069–1075, 1997.

[74] C.-s. R. Li, X. Luo, R. Sinha, B. J. Rounsaville, K. M. Carroll, R. T. Malison, Y.-S. Ding, S. Zhang, and J. S. Ide, "Increased error-related thalamic activity during early compared to late cocaine abstinence," *Drug and alcohol dependence*, vol. 109, no. 1, pp. 181–189, 2010.

[75] K. Somasundaram and S. Gayathri, "Brain segmentation in magnetic resonance images using fast fourier transform," in *Emerging Trends in Science, Engineering and Technology (INCOSET), 2012 International Conference on*. IEEE, 2012, pp. 164–168.

[76] J. P. Chiverton and K. Wells, "Adaptive partial volume classification of MRI data," *Physics in Medicine and Biology*, vol. 53, no. 20, pp. 5577–5594, 2008.

[77] P. C. Teo, G. Sapiro, and B. A. Wandell, "Creating connected representations of cortical gray matter forfunctional MRI visualization," *IEEE Transactions on Medical Imaging*, vol. 16, no. 6, pp. 852–863, 1997.

[78] D. L. Collins, A. P. Zijdenbos, V. Kollokian, J. G. Sled, N. J. Kabani, C. J. Holmes, and A. C. Evans, "Design and construction of a realistic digital brain phantom," *IEEE Transactions on Medical Imaging*, vol. 17, no. 3, pp. 463–468, 1998.

[79] S. K. Warfield, K. H. Zou, and W. M. Wells, "Simultaneous truth and performance level estimation (STAPLE): an algorithm for the validation of image segmentation," *IEEE Transactions on Medical Imaging*, vol. 23, no. 7, pp. 903–921, 2004.

[80] S. Bouix, M. Martin-Fernandez, L. Ungar, M. Nakamura, M. S. Koo, R. W. McCarley, and M. E. Shenton, "On evaluating brain tissue classifiers without a ground truth," *Neuroimage*, vol. 36, no. 4, pp. 1207–1224, 2007.

[81] R. L. Chiang-shan, X. Luo, R. Sinha, B. J. Rounsaville, K. M. Carroll, R. T. Malison, Y.-S. Ding, S. Zhang, and J. S. Ide, "Increased error-related thalamic activity during early compared to late cocaine abstinence," *Drug and alcohol dependence*, vol. 109, no. 1, pp. 181–189, 2010.

[82] F. A. M. Cappabianco, J. S. Ide, A. X. Falcão, and C. shan R. L., "Automatic Subcortical Tissue Segmentation of MR Images Using Optimum-Path Forest Clustering," in *IEEE ICIP*, 2011, pp. 2709–2712.

[83] P. A. V. Miranda, A. X. Falcão, and J. K. Udupa, "Cloud bank: A multiple clouds model and its use in MR brain image segmentation," in *IEEE ISBI*, June 2009, pp. 506–509.

[84] A. A. Taha and A. Hanbury, "Metrics for evaluating 3d medical image segmentation: analysis, selection, and tool," *BMC medical imaging*, vol. 15, no. 1, p. 29, 2015.

[85] N. Gordillo, E. Montseny, and P. Sobrevilla, "State of the art survey on mri brain tumor segmentation," *Magnetic resonance imaging*, vol. 31, no. 8, pp. 1426–1438, 2013.

[86] J. Ashburner and C. D. Good, "Spatial registration of images," in *Quantitative MRI of the Brain: Measuring Changes Caused by Disease*, P. Tofts, Ed. John Wiley & Sons, 2003, ch. 15, pp. 503–532.

[87] T. M. Lehmann, C. Gonner, and K. Spitzer, "Survey: Interpolation methods in medical image processing," *IEEE TRANSACTIONS ON MEDICAL IMAGING*, vol. 18, no. 11, pp. 1049–1075, 1999.

[88] E. H. W. Meijering, "Spline interpolation in medical imaging: comparison with other convolution-based approaches," *Proceedings of EUSIPCO 2000, M. Gabbouj and P. Kuosmanen (eds.)*, vol. IV, pp. 1989–1996, 2000.

[89] A. Amanatiadis and I. Andreadis, "A survey on evaluation methods for image interpolation," *Measurement Science and Technology*, vol. 20, no. 10, p. 104015, 2009.

[90] P. A. Miranda, F. A. Cappabianco, and J. S. Ide, "A case analysis of the impact of prior center of gravity estimation over skull-stripping algorithms in mr images," in *2013 IEEE International Conference on Image Processing*. IEEE, 2013, pp. 675–679.

[91] M. Brett, I. S. Johnsrude, and A. M. Owen, "The problem of functional localization in the human brain," *Nature reviews neuroscience*, vol. 3, no. 3, pp. 243–249, 2002.

[92] A. Klein, J. Anderssonb, B. A. Ardekani, J. Ashburner, B. Avants, M.-C. Chiang, G. E. Christensen, D. L. Collins, J. Gee, P. Hellier, J. H. Song, M. Jenkinson, C. Lepage, D. Rueckert, P. Thompson,

T. Vercauteren, R. P. Woods, J. J. Mann, and R. V. Parsey, "Evaluation of 14 nonlinear deformation algorithms applied to human brain mri registration," *NeuroImage*, vol. 46, no. 3, p. 786802, 2009.

[93] M. Jenkinson, C. F. Beckmann, T. E. Behrens, M. W. Woolrich, and S. Smith, "Fsl," *NeuroImage*, vol. 62, no. 2, pp. 782–790, 2001.

[94] J. L. Andersson, M. Jenkinson, S. Smith *et al.*, "Non-linear registration, aka spatial normalisation fmrib technical report tr07ja2," *FMRIB Analysis Group of the University of Oxford*, vol. 2, 2007.

[95] B. B. Avants, N. Tustison, and G. Song, "Advanced normalization tools (ants)," *Insight J*, vol. 2, pp. 1–35, 2009.

[96] N. J. Tustison, P. A. Cook, A. Klein, G. Song, S. R. Das, J. T. Duda, B. M. Kandel, N. van Strien, J. R. Stone, J. C. Gee *et al.*, "Large-scale evaluation of ants and freesurfer cortical thickness measurements," *Neuroimage*, vol. 99, pp. 166–179, 2014.

[97] S. Klein, M. Staring, K. Murphy, M. A. Viergever, and J. P. Pluim, "Elastix: a toolbox for intensity-based medical image registration," *IEEE transactions on medical imaging*, vol. 29, no. 1, pp. 196–205, 2010.

[98] J. West and et al., "Comparison and evaluation of retrospective intermodality brain image registration techniques," *Journal of Computer Assisted Tomography*, vol. 21, no. 4, pp. 554–566, 1997.

[99] M. Jenkinson and S. Smith, "A global optimisation method for robust affine registration of brain images," *Medical Image Analysis*, vol. 5, pp. 143–156, 2001.

[100] M. Jenkinson, P. Bannister, M. Brady, and S. Smith, "Improved optimization for the robust and accurate linear registration and motion correction of brain images," *Neuroimage*, vol. 17, no. 2, pp. 825–841, 2002.

[101] J. Ide, S. Zhang, and C. Li, "Bayesian network models in brain functional connectivity analysis," *International Journal of Approximate Reasoning*, vol. 55, no. 1, Part 1, pp. 23–35, 2014.

[102] S. Ogawa, T. M. Lee, A. R. Kay, and D. W. Tank, "Brain magnetic resonance imaging with contrast dependent on blood oxygenation," *Proc Natl Acad Sci U S A*, vol. 87, no. 24, pp. 9868–72, 1990. [Online]. Available: http://www.ncbi.nlm.nih.gov/entrez/query.fcgi?cmd=Retrieve&db=PubMed&dopt=Citation&list_uids=2124706

[103] S. A. Huettel, A. W. Song, and G. McCarthy, *Functional Magnetic Resonance Imaging*, 2nd ed. Sinauer, 2009.

[104] M. D. Fox, A. Z. Snyder, J. L. Vincent, M. Corbetta, D. C. Van Essen, and M. E. Raichle, "The human brain is intrinsically organized into dynamic, anticorrelated functional networks," *Proc Natl Acad Sci U S A*, vol. 102, no. 27, pp. 9673–8, 2005. [Online]. Available: http://www.ncbi.nlm.nih.gov/entrez/query.fcgi?cmd=Retrieve&db=PubMed&dopt=Citation&list_uids=15976020

[105] B. B. Biswal, M. Mennes, X. N. Zuo, S. Gohel, C. Kelly, S. M. Smith, C. F. Beckmann, J. S. Adelstein, R. L. Buckner, S. Colcombe, A. M. Dogonowski, M. Ernst, D. Fair, M. Hampson, M. J. Hoptman, J. S. Hyde, V. J. Kiviniemi, R. Kotter, S. J. Li, C. P. Lin, M. J. Lowe, C. Mackay, D. J. Madden, K. H. Madsen, D. S. Margulies, H. S. Mayberg, K. McMahon, C. S. Monk, S. H. Mostofsky, B. J. Nagel, J. J. Pekar, S. J. Peltier, S. E. Petersen, V. Riedl, S. A. Rombouts, B. Rypma, B. L. Schlaggar, S. Schmidt, R. D. Seidler, G. J. Siegle, C. Sorg, G. J. Teng, J. Veijola, A. Villringer, M. Walter, L. Wang, X. C. Weng, S. Whitfield-Gabrieli, P. Williamson, C. Windischberger, Y. F. Zang, H. Y. Zhang, F. X. Castellanos, and M. P. Milham, "Toward discovery science of human brain function," *Proc Natl Acad Sci U S A*, vol. 107, no. 10, pp. 4734–9, 2010. [Online]. Available: http://www.ncbi.nlm.nih.gov/entrez/query.fcgi?cmd=Retrieve&db=PubMed&dopt=Citation&list_uids=20176931

[106] K. Friston, "Functional and effective connectivity: A review," *Brain Connectivity*, vol. 1, no. 1, pp. 13–36, 2011.

[107] B. Biswal, F. Z. Yetkin, V. M. Haughton, and J. S. Hyde, "Functional connectivity in the motor cortex of resting human brain using echo-planar mri," *Magn Reson Med*, vol. 34, no. 4, pp. 537–41, 1995. [Online]. Available: http://www.ncbi.nlm.nih.gov/entrez/query.fcgi?cmd=Retrieve&db=PubMed&dopt=Citation&list_uids=8524021

[108] A. Roebroeck, E. Formisano, and R. Goebel, "Mapping directed influence over the brain using granger causality and fmri," *Neuroimage*, vol. 25, no. 1, pp. 230–42, 2005. [Online]. Available: http://www.ncbi.nlm.nih.gov/entrez/query.fcgi?cmd=Retrieve&db=PubMed&dopt=Citation&list_uids=15734358

[109] K. J. Friston, C. Buechel, G. R. Fink, J. Morris, E. Rolls, and R. J. Dolan, "Psychophysiological and modulatory interactions in neuroimaging," *Neuroimage*, vol. 6, no. 3, pp. 218–29, 1997. [Online]. Available: http://www.ncbi.nlm.nih.gov/entrez/query.fcgi?cmd=Retrieve&db=PubMed&dopt=Citation&list_uids=9344826

[110] A. R. McIntosh and F. Gonzalez-Lima, "Structural equation modeling and its application to network analysis in functional brain imaging," *Human Brain Mapping*, vol. 2, no. 1-2, pp. 2–22, 1994. [Online]. Available: http://dx.doi.org/10.1002/hbm.460020104

[111] G. Deshpande, S. LaConte, G. A. James, S. Peltier, and X. Hu, "Multivariate granger causality analysis of fmri data," *Hum Brain Mapp*, vol. 30, no. 4, pp. 1361–73, 2009. [Online]. Available: http://www.ncbi.nlm.nih.gov/entrez/query.fcgi?cmd=Retrieve&db=PubMed&dopt=Citation&list_uids=18537116

[112] K. J. Friston, L. Harrison, and W. Penny, "Dynamic causal modelling," *NeuroImage*, vol. 19, no. 4, p. 1273, 2003. [Online]. Available: http://www.sciencedirect.com/science/article/B6WNP-490RDHC-7/2/f2b9487cbf5512315e4bc9980554cde3

[113] M. J. McKeown, S. Makeig, G. G. Brown, T. P. Jung, S. S. Kindermann, A. J. Bell, and T. J. Sejnowski, "Analysis of fmri data by blind separation into independent spatial components," *Hum Brain Mapp*, vol. 6, no. 3, pp. 160–88, 1998. [Online]. Available: http://www.ncbi.nlm.nih.gov/entrez/query.fcgi?cmd=Retrieve&db=PubMed&dopt=Citation&list_uids=9673671

[114] G. Deshpande, P. Santhanam, and X. Hu, "Instantaneous and causal connectivity in resting state brain networks derived from functional mri data," *Neuroimage*, vol. 54, no. 2, pp. 1043–52, 2011. [Online]. Available: http://www.ncbi.nlm.nih.gov/entrez/query.fcgi?cmd=Retrieve&db=PubMed&dopt=Citation&list_uids=20850549

[115] J. Ide and C. Li, "Error-related functional connectivity of the habenula in humans," *Frontiers in Human Neuroscience*, vol. 5, 2011. [Online]. Available: http://www.frontiersin.org/Journal/Abstract.aspx?s=537&name=humanneuroscience&ART_DOI=10.3389/fnhum.2011.00025

[116] S. M. Smith, K. L. Miller, G. Salimi-Khorshidi, M. Webster, C. F. Beckmann, T. E. Nichols, J. D. Ramsey, and M. W. Woolrich, "Network modelling methods for fmri," *Neuroimage*, vol. 54, no. 2, pp. 875–91, 2011. [Online]. Available: http://www.ncbi.nlm.nih.gov/entrez/query.fcgi?cmd=Retrieve&db=PubMed&dopt=Citation&list_uids=20817103

[117] J. D. Ramsey, S. J. Hanson, C. Hanson, Y. O. Halchenko, R. A. Poldrack, and C. Glymour, "Six problems for causal inference from fmri," *NeuroImage*, vol. In Press, Corrected Proof, 2010. [Online]. Available: http://www.sciencedirect.com/science/article/B6WNP-4X66S4F-1/2/95836b14a46af70b2676b57399e2c0b4

[118] M. A. Lindquist and M. E. Sobel, "Cloak and dag: A response to the comments on our comment," *Neuroimage*, (in press). [Online]. Available: http://www.ncbi.nlm.nih.gov/entrez/query.fcgi?cmd=Retrieve&db=PubMed&dopt=Citation&list_uids=22119004

[119] G. K. Aguirre, E. Zarahn, and M. D'Esposito, "The variability of human, bold hemodynamic responses," *Neuroimage*, vol. 8, no. 4, pp. 360–9, 1998. [Online]. Available: http://www.ncbi.nlm.nih.gov/entrez/query.fcgi?cmd=Retrieve&db=PubMed&dopt=Citation&list_uids=9811554

[120] G. Deshpande and X. Hu, "Investigating effective brain connectivity from fmri data: Past findings and current issues with reference to granger causality analysis," *Brain Connectivity*, vol. 2, no. 5, pp. 235–245, 2012. [Online]. Available: http://www.ncbi.nlm.nih.gov/pmc/articles/PMC3621319/

[121] K. J. Friston, "Modalities, modes, and models in functional neuroimaging," *Science*, vol. 326, no. 5951, pp. 399–403, 2009.

[122] J. D. Haynes and G. Rees, "Decoding mental states from brain activity in humans," *Nat Rev Neurosci*, vol. 7, no. 7, pp. 523–34, 2006.

[123] J. Schrouff, M. J. Rosa, J. M. Rondina, A. F. Marquand, C. Chu, J. Ashburner, C. Phillips, J. Richiardi, and J. Mourao-Miranda, "Pronto: pattern recognition for neuroimaging toolbox," *Neuroinformatics*, vol. 11, no. 3, pp. 319–37, 2013.

[124] M. Hanke, Y. O. Halchenko, P. B. Sederberg, S. J. Hanson, J. V. Haxby, and S. Pollmann, "Pymvpa: a python toolbox for multivariate pattern analysis of fmri data," *Neuroinformatics*, vol. 7, no. 1, pp. 37–53, 2009.

[125] J. Honorio, "Classification on brain functional magnetic resonance imaging:: dimensionality, sample size, subject variability and noise," in *Frontiers of Medical Imaging*, C. Chen, Ed. World Scientific Publishing Company Pte Limited, 2014, ch. 14, pp. 266–290.

[126] F. Faria, F. Cappabianco, C. Li, and J. Ide, "Information fusion for cocaine dependence recognition using fmri," *In: 23rd International Conference on Pattern Recognition, 2016, Cancun.*, (in press).